Bioactivation of the Fungal Phytotoxin 2,5-Anhydro-D-glucitol by Glycolytic Enzymes is an Essential Component of its Mechanism of Action

Franck E. Dayan[a,*], Agnes M. Rimando[a], Mario R. Tellez[a], Brian E. Scheffler[a], Thibaut Roy[b], Hamed K. Abbas[c] and Stephen O. Duke[a]

[a] USDA-ARS Natural Products Utilization Research Unit, P.O. Box 8048, University, MS 38677, USA. Fax 662-915-1035. E-mail: fdayan@ars.usda.gov
[b] Laboratoire de Biologie Moléculaire et Cellulaire, Université de Bourgogne, 21000 Dijon, France
[c] USDA-ARS Crop Genetics & Production Research Unit, P.O. Box 350, Stoneville, MS 38776, USA

* Author for correspondence and reprint requests

Z. Naturforsch. **57c,** 645–653 (2002); received February 27/March 27, 2002

Bioactivation of Phytotoxin, Plant/Pathogen Interaction, Inhibition of Aldolase

An isolate of *Fusarium solani*, NRRL 18883, produces the natural phytotoxin 2,5-anhydro-D-glucitol (AhG). This fungal metabolite inhibited the growth of roots (I_{50} of 1.6 mM), but it did not have any *in vitro* inhibitory activity. The mechanism of action of AhG requires enzymatic phosphorylation by plant glycolytic kinases to yield AhG-1,6-bisphosphate (AhG-1,6-bisP), an inhibitor of Fru-1,6-bisP aldolase. AhG-1,6-bisP had an I_{50} value of 570 μM on aldolase activity, and it competed with Fru-1,6-bisP for the catalytic site on the enzyme, with a K_i value of 103 μM. The hydroxyl group on the anomeric carbon of Fru-1,6-bisP is required for the formation of an essential covalent bond to ζ amino functionality of lysine 225. The absence of this hydroxyl group on AhG-1,6-bisP prevents the normal catalytic function of aldolase. Nonetheless, modeling of the binding of AhG-1,6-bisP to the catalytic pocket shows that the inhibitor interacts with the amino acid residues of the binding site in a manner similar to that of Fru-1,6-bisP. The ability of *F. solani* to produce a fructose analog that is bioactivated by enzymes of the host plant in order to inhibit a major metabolic pathway illustrates the intricate biochemical processes involved in plant-pathogen interactions.

Introduction

Interactions between pathogenic fungi and their host plants involve complex physical and chemical communications that lead to a series of actions and reactions by both the infecting microorganisms and the plants being infected (Fray *et al.*, 1999; Pedras *et al.*, 2001; Vera-Estrella *et al.*, 1994). The virulence of an organism is sometimes enhanced by its ability to produce phytotoxins that kill cells in the tissue surrounding the point of infection (Baker *et al.*, 1997). Fungi and other microorganisms that produce such biochemical compounds (or phytochemicals) are being studied as potential biocontrol agents for weed management. These studies have led to the discovery of many pathogenic *Fusarium* spp., such as *F. oxysporum* and *F. moniliforme*, that can be used to control a broad range of weed species (Abbas *et al.*, 1991, 1996; Abbas and Boyette, 1992; Boyette *et al.*, 1993). Moreover, studies on the pathogenicity of fungi from this genus have resulted in the isolation and identification of many potent natural phytotoxins such as fumonisins, moniliformin, fusaric acid and trichothecenes (Abbas *et al.*, 1991; Abbas and Boyette, 1992; Boyette *et al.*, 1993; Jin *et al.*, 1996). These natural toxins play important roles in inhibiting the physiological processes in cells surrounding the point of infection, enabling the spread of the disease (Feys and Parker, 2000; Staskawicz *et al.*, 2001).

The natural product 2,5-anhydro-D-glucitol (AhG) (Fig. 1A) was isolated from the fungal pathogen *Fusarium solani* (Mart.) Sacc. NRRL 18883 that was highly phytotoxic on several plant species (Tanaka *et al.*, 1996). Objectives of the work reported here are to determine the mechanism of action and to understand the role of this

AhG, 2,5-anhydro-D-glucitol; AhG-P, 2,5-anhydro-D-glucitol-monophosphate; AhG-1,6-bisP, 2,5-anhydro-D-glucitol-1,6-bisphosphate; Fru-1,6-bisP, Fructose-1,6-bisphosphate; PFK, phosphofructokinase; PAR, photosynthetically active radiation.

 © 2002 Verlag der Zeitschrift für Naturforschung, Tübingen · www.znaturforsch.com ·

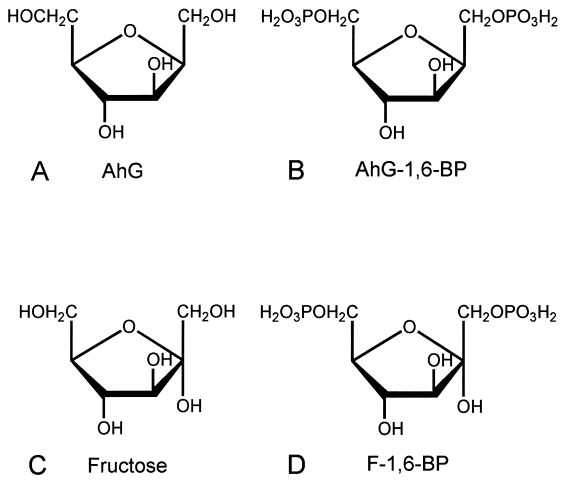

Fig. 1. Chemical structure of (A) AhG, (B) AhG-BP, (C) fructose, and (D) Fru-1,6-bisP.

structural analog of Fru (Fig. 1C) in the virulence of this strain of *F. solani*.

Plant aldolases are class-I type enzymes that possess a key lysine residue in the catalytic site required for the formation of a covalent intermediate in the form of a Schiff base with its substrate prior to the aldol cleavage (Anderson and Advani, 1970). As such, plant aldolases have similar reaction mechanisms as other class-I aldolases. Plants have cytoplasmic and chloroplastic isozymes that exist as homotetramers with native molecular masses of approximately 140 kDa (Lebherz *et al.*, 1984; Pelzer-Reith *et al.*, 1993). While the sequence and structure of the isoforms are related (Marshall *et al.*, 1989), the chloroplastic isozyme has a transit peptide and a different substrate specificity (Krüger and Schnarrenberger, 1983). Fru-1,6-bisP aldolase (EC 4.1.2.13) catalyzes the reversible aldol cleavage of Fru-1,6-bisP into glyceraldehyde-3-phosphate (G-3-P) and dihydroxyacetone phosphate (ΔHAP). Inhibition of this step of glycolysis is known to have long-ranging repercussions on the overall physiology of plants, leading to reduced photosynthetic efficiency, impaired sugar and starch metabolism, and ultimately reduced growth (Haake *et al.*, 1998).

This study found that the fungal metabolite AhG has a novel mechanism of action requiring enzymatic bioactivation via phosphorylation by glycolytic kinases to form 2,5-anhydro-D-glucitol-1,6-bisphosphate (AhG-1,6-bisP) (Fig. 1B). This bioactivated phytotoxin competitively inhibits Fru-1,6-bisP aldolase.

Materials and Methods

Production, extraction, and purification of AhG

F. solani NRRL 18883 was grown on solid rice medium as described by Abbas *et al.* (1991). Rice grains were inoculated with the fungus and incubated for 21 days at 20 to 22 °C. Cultures were then air dried and powdered with a Stein Mill grinder. Isolation of AhG was performed in a bioassay-guided manner using various chromatographic procedures. The powder was extracted exhaustively with MeOH and subsequently concentrated under vacuum and partitioned with hexane. The MeOH fraction was found to be highly phytotoxic, whereas the hexane fraction lacked activity. The MeOH fraction was chromatographed over a Diaion-HP 20 resin (Supelco, Bellefonte, PA) column eluted with 500 ml each of varying proportions of H_2O:MeOH and MeOH:CH_2Cl_2. Phytotoxic activity was found in the fraction eluted with 80:20 v/v H_2O:MeOH and 60:40 v/v H_2O:MeOH. These fractions were combined and chromatographed on a silica gel (Mallinckrodt Chemical, Paris, KY) column eluted with combination of hexane:CH_2Cl_2, CH_2Cl_2:MeOH, and finally with 100% MeOH. Phytotoxic activity was shown in the fraction eluted with 50:50 v/v CH_2Cl_2:MeOH. This fraction was subjected to further chromatographic separation using a reversed-phase preparative column, Lichroprep RP-8 (E. M. Science, Gibbstown, NJ) eluting with H_2O:MeOH in increasing proportion of MeOH. AhG eluted with 95:5 H_2O:MeOH. The structure of AhG was confirmed by ^1H and ^{13}C NMR and by GC-MS (Tanaka *et al.*, 1996) . The phosphorylated analog, AhG-1,6-bisP, was purchased from Toronto Research Chemicals Inc. (North York, Ontario, Canada).

Phytotoxicity of AhG and AhG-1,6-bisP

The natural toxin AhG and its phosphorylated AhG-1,6-bisP analog were tested for herbicidal activity. Biological activity was tested on lettuce (*Lactuca sativa* cv. Iceberg) in 6-cm disposable petri dishes. Each treatment consisted of 3 replicates with 25 observations each (n = 75). Test com-

pounds were dissolved in water and tested at final concentrations up to 6 mM. Controls consisted of seeds germinated without the test compounds. Plates were incubated at 25 ± 2 °C under cool white fluorescent lights maintaining a 16-h photoperiod at 400 μmol m^{-2} s^{-1} photosynthetically active radiation (PAR). The overall appearance of the seedlings and their root lengths were measured after 7 d of growth as described in Dayan *et al.* (2000).

Biological phosphorylation of AhG

Enzymatic phosphorylation of AhG was determined *in vitro*. Bisphosphorylation of AhG at carbons 1 and 6 to form AhG-1,6-bisP by hexokinase and phosphofructosekinase (PFK) was measured in crude cell-free spinach extracts. A crude cytosolic extract containing the enzymes hexokinase and PFK was obtained from leaves of spinach by modifying the method of Morrell and Rees (1986). The protein extract was desalted on a PD-10 column to remove endogenous sugars and other small molecules that would interfere with the detection of AhG and the phosphorylated analogs. The reaction mixture contained 10 mM AhG, 5 mM Hepes (*N*-[2-hydroxyethyl]piperazine-*N*′-[2-ethanesulfonic acid]) (pH 7.0), 5 mM $MgCl_2$, 10 mM ATP and 10 mg/ml protein from the spinach extract. The mixture was incubated for 4 h at 25 °C. The enzyme was removed from the solution by centrifugation using a centricon YM-30 spin column at 7000 × *g* for 10 min. The presence of AhG, AhG-P, and AhG-1,6-bisP was detected by mass spectrometry by direct injection in a LCQ mass spectrometer (ThermoQuest, San Jose, CA) equipped with electrospray ionization (ESI) in the negative mode.

Inhibition of plant aldolase

Aldolase activity was determined by coupling the aldolase assay with an α-glycerophosphate dehydrogenase assay, and monitoring the decrease in NADH concentration at A_{340}. The assay buffer consisted of 50 mM Tris-HCl (tris(hydroxymethyl) aminomethane hydrochloride), pH 8 with 3 mM $MgCl_2$. The I_{50} values (concentration of inhibitor required for 50 percent inhibition of aldolase activity), of AhG and AhG-1,6-bisP on spinach aldolase was determined by testing the inhibitors at 0.10, 0.33, 0.55, 0.66, 0.88 and 1.00 mM. Spinach aldolase (2.4 unit/ml) was incubated with the compounds for 15 minutes on ice prior to assay. The aldolase sample (100 μl) was mixed with 800 μl of the reaction assay containing 0.15 mM NADH, 1 unit/ml triosephosphate isomerase and 0.1 unit/ml glycerol-3-phosphate dehydrogenase in 50 mM Tris-HCl, pH 8 (one unit of triosephosphate isomerase converts 1.0 μmol D-glyceraldehyde-3-phosphate to dihydroxyacetone phosphate min^{-1}, and one unit of glycerol-3-phosphate dehydrogenase converts 1.0 μmol of dihydroxyacetone phosphate to α-glycerophosphate min^{-1} at pH 7.4). The reaction was initiated by the addition of 100 μl of Fru-1,6-bisP to obtain a 333 μM final concentration. The reaction was incubated at 30 °C for 1 minute prior to measurement of change in A_{340} in a Shimadzu model UV3101PC spectrophotometer with the cell thermostabilized at 30 °C.

Initial kinetic studies used Fru-1,6-bisP concentrations ranging from 10 and 333 μM and the K_m and V_{max} were determined on a Lineweaver and Burk reciprocal plot as implemented in Kinetic module of Sigma Plot 2001 for Windows, version 7.0. The type of inhibition associated with AhG-1,6-bisP was tested by repeating the kinetic measurements in the presence of 100 and 200 μM of the phosphorylated inhibitor. Since AhG did not inhibit spinach aldolase in the dose-response assays, this compound was not further evaluated in the kinetic experiments. The K_i value was calculated by a Dixon plot.

Modeling of the binding of AhG-1,6-bisP to spinach aldolase

MegAlign version 5.01 of the Lasergene suite by DNASTAR, Inc. Madison, WI USA 2001 was used to download the spinach cytoplasmic Fru-1,6-bisP aldolase protein sequence (accession P29356) and the built-in Blastp function was used to search for homology in the NCBI protein database. A total of 36 protein sequences were downloaded (10 plant cytoplasmic, 11 plant chloroplastic, and 15 animal) and aligned using the Clustal W algorithm. Each sequence was compared individually to the spinach sequence to determine the percentage of amino acid identity.

The X-ray crystal coordinates of Fru-1,6-bisP aldolases were obtained from the Brookhaven Pro-

tein Database. Since a crystal structure of plant aldolase is not available, the following structures were selected for homology modeling: The crystal structure of human Fru-1,6-bisP aldolase without the substrate (1ALD.pdb) at a resolution of 2.0 Å from Gamblin *et al.* (1991) and with the substrate (4ALD.pdb) at a resolution of 2.8 Å from Dalby *et al.* (1999).

The significant sequence homology between spinach aldolase (Pelzer-Reith *et al.*, 1993) and aldolase of other organisms (as discussed later) enabled the construction of a homology model of the spinach Fru-1,6-bisP aldolase using the modeling software COMPOSER in Sybyl 6.7 (Tripos associates, St Louis, MO) on a Silicon Graphics O_2 250 MHz R10000 workstation. This software enables knowledge-based homology modeling of protein by following a stepwise approach. In brief, the sequences are aligned, significantly conserved regions are assigned to seed residues topologically equivalent across the sequences and a model backbone is constructed. Structurally variable regions are then constructed and modeled based on the similarity to other sequences in the database. Proline Φ angles were fixed at 70 degrees, side chain amides were checked to maximize potential H-bonding, side chains were checked for close van der Waals contacts, and essential hydrogens were added. The model was checked for conformational problems using the module ProTable from Sybyl. Ramachandran plot, local geometry and the location of buried polar residues/exposed non-polar residues were examined. The model was then subjected to energy minimization following the gradient termination of the Powell method for 3000 iterations using Kollman united force field with NB cutoff set at 9.0 and the dielectric constant set at 4.0.

Structures of AhG, Fru, and various phosphorylated intermediates were built based on the X-ray crystal of Fru (Cambridge). The binding of either the natural substrate Fru-1,6-bisP or the inhibitor AhG-1,6-bisP was adjusted within the binding site using the FlexiDock module of Sybyl 6.7. The ligands, either Fru-1,6-bisP or AhG-1,6-bisP, were prepositioned in the binding pocket by approximating the coordinates of the linearized Fru-1,6-bisP available in the crystal structure of human aldolase 4ALD.pdb. The binding pocket was defined by selecting all the residues within a 3 Å boundary around the ligand. Briefly, partial charges were assigned to the atoms. All donor and receptor atoms and rotatable bonds were selected in the binding pocket and the ligands to optimize the interaction. The distances between atoms involved in hydrogen bonding in the ligand/receptor interaction were measured in the resulting models.

Results

Phytotoxicity of AhG and AhG-1,6-bisP

The natural fungal phytotoxin AhG was moderately active on the root growth of lettuce seedlings. The I_{50} of this compound was 1.6 mM. Total inhibition of root growth was caused by 3 mM (Fig. 2), whereas the bisphosphorylated AhG-1,6-bisP was not active on the growth of the seedlings. AhG-treated seedlings were smaller in overall size and leaves exhibited necrosis and chlorosis.

Biological phosphorylation of AhG

A crude cell-free cytosolic extract of spinach leaves, containing hexokinase and PFK activity, utilized AhG as a substrate and sequentially phosphorylated to form AhG-P and AhG-1,6-bisP. The *in vivo* conversion was essentially complete after 4 h incubation and was detected by the decrease of the signal for AhG (m/z = 163 [M^{-1}]) and the

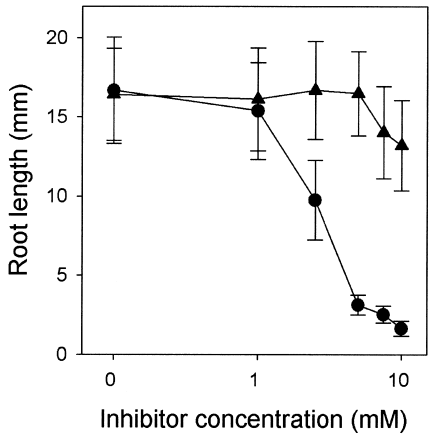

Fig. 2. Phytotoxicity of AhG (●) and AhG-BP (▲) on lettuce seedlings. Root length of seedlings were measured after 7 d of growth 25 ± 2 °C with a 16-h photoperiod at 400 μmol m^{-2} s^{-1} PAR. 25 roots were measured at each concentration and the experiment was repeated 3 times.

appearance of clear signals for AhG-P (m/z = 243 [M^{-1}]) and AhG-1,6-bisP (m/z = 323 [M^{-1}]).

Inhibition of spinach Fru-1,6-bisP aldolase

AhG-1,6-bisP inhibited the activity of spinach Fru-1,6-bisP aldolase in a dose-dependent manner. Its I_{50} value was 570 μM (Fig. 3A). The level of inhibition was not dependent on the time of incubation, suggesting that the binding of the AhG-1,6-bisP was reversible. On the other hand, AhG had no inhibitory effect on aldolase activity.

The spinach aldolase preparation used in this study had a K_m of 26 μM and V_{max} of 1.5 × 10^{-2} μM min^{-1} for Fru-1,6-bisP (Fig. 3B). Kinetic analysis of spinach aldolase activity in the presence of either 100 or 200 μM AhG-1,6-bisP indicated that this substrate analog behaved as a competitive inhibitor of the enzyme (Fig. 3B). The K_i of AhG-1,6-bisP on aldolase was 103 μM, as determined on a Dixon plot of the kinetic data.

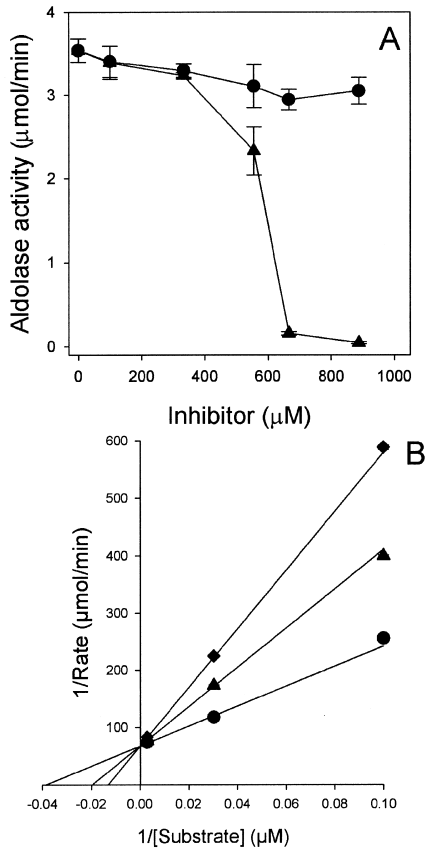

Fig. 3. A) Inhibitory activity of AhG (●) and AhG-BP (▲) on spinach Fru-1,6-bisP aldolase. B) Kinetic of spinach aldolase activity in the presence of 0 (●), 100 (▲) and 200 μM (■) AhG-BP. All assays were performed in 50 mM Tris-HCl, pH 8 with 3 mM $MgCl_2$ at 30 °C.

Modeling of spinach aldolase and the binding of AhG-1,6-bisP to the catalytic site

The homology between the amino acid sequence of spinach cytosolic aldolase and 9 other plant cytosolic aldolases ranged from 64.3 to 90.8% amino acid identity. The sequence homology was significantly less with the 11 chloroplastic aldolase sequences available, ranging from 51.7 to 59.8% amino acid identity. Interestingly, spinach cytosolic aldolase has a greater sequence homology to the 10 available animal aldolases sequences than to chloroplastic ones, ranging from 59.1–62.5%.

No crystal structure was available for plant aldolase. The published structures of human Fru-1,6-bisP aldolase 1ALD.pdb and 4ALD.pdb were selected because of the resolution of the crystals and the high degree of sequence homology (62%) to the plant sequence. These crystal structures were used to model the 3-dimensional conformation of spinach aldolase. Examination of the model indicated that the proline angles and the amide side chains were within normal range. However, when adding the side chains, the phenyl rings of tyr246 and phe264 occupied the same molecular space. The loop containing tyr246 was remodeled to allow for the presence of the side chain of tyrosine. After making this adjustment, the model did not contain other problematic regions.

The model was analyzed to assess the quality of the structure by checking the geometry and stereochemistry, solvent accessible surface areas, side chain conformational probabilities, and backbone and side chain conformation. No major discrepancies were found. A Ramachandran plot of the model indicated that, as expected, most Φ angles are negative and Ψ angles are positive. The few outliers with positive Φ were mostly glycine residues that are not subject to the strong conformational constraints due to a lack of a side chain. Analysis of the Ramachandran plot showed 95% of the non-glycine residues in 'most favored regions'. Alignment of the homology model to crystal structure of 1ALD.pdb has a root mean square

distance of 1.714 Å, underlining the high degree of similarity between the two enzymes (Fig. 4A).

Binding of Fru-1,6-bisP and AhG-1,6-bisP modeled by FlexiDock provided an estimation of the

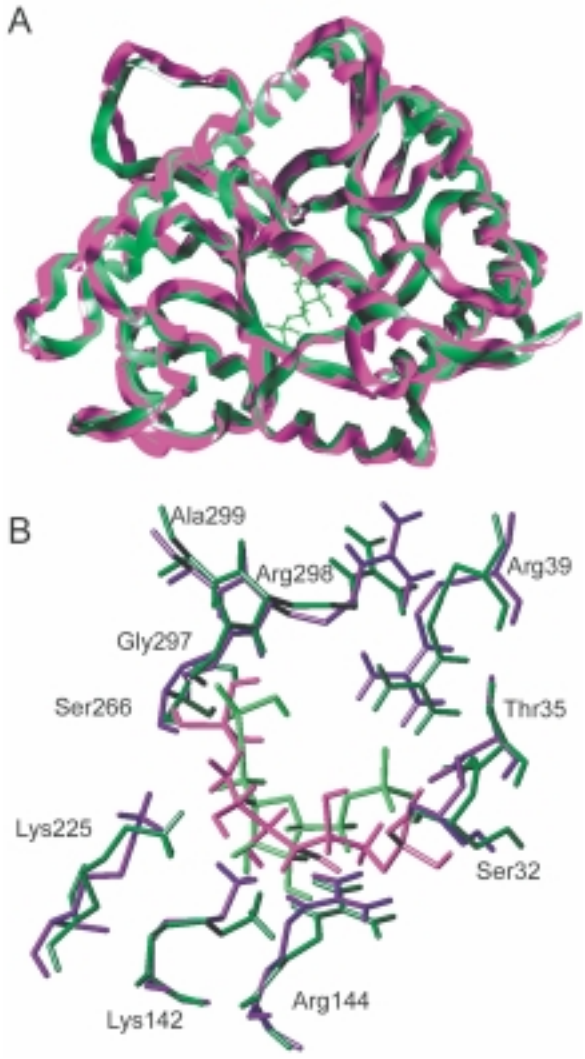

Fig. 4. Homology model of spinach cytosolic Fru-1,6-bisP aldolase and the binding of AhG-BP to the catalytic site. A) Overlay of spinach Fru-1,6-bisP aldolase (green) and the crystal structure of human Fru-1,6-bisP aldolase (purple). AhG-BP is displayed (green) to identify the location of the catalytic site; B) Binding of the bioactivated fungal toxin AhG-BP (light-green) in the catalytic site of the plant aldolase (dark-green) obtained with FlexiDock overlayed on the crystal structure of the human aldolase (purple) with Fru-1,6-bisP in its linear form (magenta). The amino acid numbering is based on the spinash sequence. Threonine 35 is a serine in the human Fru-1,6-bisP aldolase sequence.

Table I. Homology between amino acid residues involved in the binding pocket of Fru-1,6-bisP aldolase, with respect to the sequence of cytosolic aldolase from spinach[a].

Residue	Conservation [%]	Other residues at that position
Ser-32	100	–
Thr-35	77.7	serine in 8 animal sequences
Arg-39	97.2	lysine in *Onchocerca volvulus*
Lys-142	100	–
Arg-144	100	–
Lys-225	100	–
Ser-266	100	–
Gly-297	72.2	alanine in all chloroplast sequences, except with the red alga *Galdieria sulphuraria*
Arg-298	100	–
Ala-299	97.2	proline in *Branchiostoma belcheri*

[a] Search for sequence homology using the Blastp function in the NCBI protein database yielded 10 plant cytosolic sequences, 11 plant chloroplast sequences and 15 animal sequences.

Table II. Close contacts (potential hydrogen bonds) between ligands and receptor site of Fru-1,6-bisP aldolase following docking using FlexiDock.

Ligand atom[b]	Protein atom	Distance, Å[a] Fru-1,6-bisP	AhG-BP
O1	Ser-266 Oη	2.62	2.57
	Arg-298 N	3.08	3.09
O2	Ser-266 Oη	2.98	2.98
	Gly-297 N	1.59	1.59
	Ala-299 N	3.14	3.16
O3	Ser-266 Oη	1.80	1.82
	Ser-266 N	1.95	1.95
	Gly-297 N	1.77	1.78
O4	Gly-297 N	3.09	3.22
O5	Lys-225 Nζ	1.82	*
O6	Arg-144 Nε	3.30	3.07
	Lys-225 Nζ	3.25	3.27
O7	Lys-142 Nζ	1.99	1.93
O10	Thr-35 Oγ1	2.19	2.01
	Arg-39 Nη1	2.63	2.62
O11	Arg-39 Nη1	1.53	1.52
	Arg-39 Nη2	1.67	1.73
O12	Ser-32 N	2.29	2.21

[a] Close contacts are distances < 3.30 Å for potential hydrogen bonding.

[b] O1, O2, and O3 are associated with the phosphate group on carbon 1, O4 is on carbon 1, O5 is on carbon 2 (anomeric), O6 is on carbon 3, O7 is on carbon 6, and O10, O11, and O12 are associated with the phosphate group on carbon 6.

* α-hydroxyl on anomeric carbon is missing in AhG-BP.

position of the ligands in the catalytic site. Most of the amino acid residues found in the binding site are highly conserved across all species known (Table I). All of the amino acid residues in the enzymatic pocket that were involved in hydrogen bonding with atoms of Fru-1,6-bisP were also participating in the stabilization of AhG-1,6-bisP (Table II). The oxygen atoms on phosphate group at carbon 1 interact with Ser-266, Gly-297, Arg-298 and Ala-299, and those of the phosphate group at carbon 6 interact with Ser-32, Thr-35 and Arg-39. The hydroxyl on the anomeric carbon of Fru-1,6-bisP interacts with the ζ amino group of Lys-225 whereas no interaction is possible at that position with AhG-1,6-bisP. While Hartman and Barker (1965) reported that the hydroxyl groups on carbons 3 and 4 are not necessary for binding to aldolase, these oxygen atoms are nonetheless within hydrogen bonding distances to the ε amino of Arg-144 and the ζ amino of Lys-142, respectively. As a result, the position of AhG in the binding pocket of the plant Fru-1,6-bisP aldolase is quite similar to that of the natural substrate in the human aldolase (Fig. 4B).

Discussion

The ability of a pathogen to infect and invade a compatible host may be facilitated by the production of toxins that induce cell death in the proximity of the invading organism (Baker *et al.*, 1997; Dangl and Jones, 2001). *Fusarium* species produce a variety of potent phytotoxins such as fumonisins, moniliformin, fusaric acid and trichothecenes (Abbas *et al.*, 1991; Abbas and Boyette, 1992; Jin *et al.*, 1996). The discovery of a strain of *F. solani* (NRRL 18883) that produced a large amounts of AhG suggested that this compound may also play a role in the virulence and symptom expression of this organism (Tanaka *et al.*, 1996).

While the phytotoxicity of exogenous application of AhG is moderate, with an I_{50} of 1.6 mM, symptoms are consistent with an overall reduction of physiological fitness. The phenotypic effect observed on seedlings treated with AhG included stunting, reduced root growth, necrosis and chlorosis. After much effort in attempting to determine the target site of AhG itself, it was discovered that this fungal metabolite was phosphorylated by the consecutive action of hexokinase and PFK, yielding AhG-1,6-bisP. This phosphorylated sugar analog did not have any *in vivo* phytotoxic activity. Uptake and translocation of this highly polar compound may be limiting factors, though one would not expect these to be major problems during the imbibition process occurring prior to seed germination in the assay. However, AhG-1,6-bisP had previously been tested as an inhibitor of aldolase in animal systems (Hartman and Barker, 1965). Therefore, it was postulated that the *in planta* release of AhG-1,6-bisP by *F. solani* may lead to cell death by inhibiting plant aldolase.

Fru-1,6-bisP aldolase reversibly catalyzes the cleavage of the Fru-1,6-bisP into the triose phosphates G-3-P and DHAP. Eukaryotic (class I) and prokaryotic (class II) aldolases exist. Class I aldolases differ from class II aldolases in that they catalyze Schiff-base formation with the substrate rather than requiring a bivalent metal ion as a cofactor (Anderson and Advani, 1970). There is a high degree of sequence homology between Class I aldolases and most of the amino acid residues involved in the catalytic site of aldolase are highly conserved (Table I).

AhG is not an appropriate substrate for aldolase because it lacks the phosphate groups involved in the positioning of the substrate in the binding pocket. On the other hand, AhG-1,6-bisP is a structural analog of Fru-1,6-bisP that binds to the catalytic site. As with Fru-1,6-bisP, the phosphate groups on carbons 1 and 6 of AhG interact with residues Ser-266, Gly-297, Arg-298 and Ala-299 or Ser-32, Thr-35 and Arg-39, respectively. It is interesting to note that domain of the binding pocket interacting with the phosphate groups of Fru-1,6-bisP and AhG-1,6-bisP have similar amino acids (serine and arginine), and that these amino acids are conserved in the sequence of all species known to date (Table I). The absence of the hydroxyl group on carbon 2, normally yielding a keto group in the linear form of Fru-1,6-bisP, prevents the initial covalent interaction between AhG-1,6-bisP and the ζ amino group of a lysine 225. This residue is involved in the formation of an iminium cation enzyme-substrate intermediate. Therefore, the phosphorylated metabolite AhG-1,6-bisP interacts with the catalytic site, but cannot undergo aldol cleavage, thereby competitively inhibiting plant aldolase (Fig. 3B). As such, it behaves in a manner similar to that observed on mammalian aldolases

(Hartman and Barker, 1965), and most other phosphorylated inhibitors of aldolase tested to date also compete for the binding site of Fru-1,6-bisP (Blonski *et al.*, 1997).

Inhibiting glycolysis at this site would be expected to have severe physiological consequences on plants. While the inhibition of aldolase by AhG-1,6-bisP is not very strong, with an I_{50} of about 570 μM and a K_i of 103 μM, it is known that small decreases in aldolase activity have strong repercussions in photosynthetic efficiency, the metabolism of sugars and starch and lead to overall growth reduction (Haake *et al.*, 1998). Therefore, the large amount of AhG produced by *F. solani* as they infect plant tissues may cause significant cellular damage and enable the rapid spread of the disease.

Knowledge-based modeling enabled the construction of a 3-dimentional model of plant aldolase. It is established that the root mean square deviation of the Cα atoms for protein sharing 40% amino acid identity is approximately 1 Å for 90% of backbone atoms (those having the most influence on the secondary and ternary conformation) (Chothia and Lesk, 1989; Sali *et al.*, 1995). Given the high similarity of the amino acid sequences of plant and human aldolases (62%) and the absence of significant conformational problems in the model, it is expected that the structure of the spinach Fru-1,6-bisP may be similar to a low resolution crystal structure of this enzyme. Furthermore, residues in the catalytic sites are extremely conserved (Table I), and the regions where the model differs from the crystal structure are in loops relatively distant from the catalytic site (Fig. 4A). The resolution of such models is generally sufficient to compare the binding of a substrate and a competitive inhibitor. As illustrated in Fig. 4B, the orientation of AhG-1,6-bisP in the binding pocket of spinach aldolase is similar to that of Fru-1,6-bisP in the mammalian catalytic site. Only minor shifts in the conformation of the amino acid side chains are necessary to accommodate the binding of the inhibitor, relative to that of Fru-1,6-bisP (Table II). In fact, the absence of the hydroxyl group on carbon 2 of AhG renders this molecule symmetrical along the axis of the oxygen bridge of the furanose ring, suggesting that the phosphorylated form of the fungal metabolite may bind to the catalytic site in either direction. It should be noted that the binding pocket also has an interesting symmetry, possessing highly conserved arginine and serine residues on either side of the receptor site that stabilize the phosphate groups (Table I and Fig. 4B).

The overall proposed mechanism of action of AhG is as follows: AhG produced by *F. solani* is probably released into the cells of the host plant. This furanose-like fungal metabolite is sequentially phosphorylated to AhG-P and AhG-1,6-bisP by the enzymatic activities of hexokinase and PFK, respectively. In this bioactivated form, AhG-1,6-bisP inhibits aldolase by competing for the binding site of Fru-1,6-bisP, which subsequently leads to the death of the cells surrounding the point of infection.

It is evident that the biochemical interactions between pathogenic microorganisms and their host plants that lead to such intricate situations are the result of a dynamic and continually evolving process. Our research effort will now focus on the quantitation of the AhG levels in infected tissues and its relationship to the virulence and pathogenicity of this organism.

Acknowledgments

We are thankful for the technical assistance of Stacy N. Allen and Susan B. Watson. This work was supported, in part, by funds from the Regional Council of Burgundy and the University of Burgundy, Faculty of Life Sciences.

Abbas H. K., Boyette C. D., Hoagland R. E. and Vesonder R. F. (1991), Bioherbicidal potential of *Fusarium moniliforme* and its phytotoxin, fumonisin. Weed Sci. **39**, 673–677.

Abbas H. K., Duke S. O., Shier W. T., Riley R. T. and Kraus G. A. (1996), The chemistry and biological activities of the natural products AAL-toxin and the fumonisins. Adv. Exp Med. Biol. **391**, 293–308.

Abbas H. K. and Boyette C. D. (1996), Control of morningglory species using *Fusarium solani* and its extracts. Internat. J. Pest. Manag. **6**, 548–552.

Anderson L. E. and Advani V. R. (1970), Chloroplast and cytoplasmic enzymes. Three distinct isoenzymes associated with the reductive pentose phosphate cycle. Plant Physiol. **45**, 583–585.

Baker B., Zambryski P., Staskawicz B. and Dinesh-Kumar S. P. (1997), Signaling in Plant-Microbe Interactions. Science **276**, 726–733.

Blonski C., De Moissac D., Périé J. and Sygusch J. (1997), Inhibition of rabbit muscle aldolase by phosphorylated aromatic compounds. Biochem. J. **323**, 71–77.

Boyette C. D., Abbas H. K. and Connick W. J. Jr. (1993), Evaluation of *Fusarium oxysporum* as a potential bioherbicide for sicklepod (*Cassia obtusifolia*), coffee senna (*C. occidentalis*), and hemp sesbania (*Sesbania exaltata*). Weed Sci. **41**, 678–681.

Chothia C. and Lesk A. M. (1989), The relation between the divergence of sequence and structure in proteins. EMBO J. **5**, 823–826.

Dalby A., Dauter Z. and Littlechild J. A. (1999), Crystal structure of human aldolase complexed with fructose-1,6-bisphosphate: mechanistic implications. Protein Sci. **8**, 291–297.

Dangl J. L. and Jones J. D. G. (2001), Plant pathogens and integrated defense responses to infection. Nature **411**, 826–833.

Dayan F. E., Romagni J. G. and Duke S. O. (2000), Investigating the mode of action of natural phytotoxins. J. Chem. Ecol. **26**, 2079–2094.

Feys B. J. and Parker J. E. (2000), Interplay of signaling pathways in plant disease resistance. Trends Genet. **16**, 449–455.

Fray R. G., Throup J. P., Daykin M., Wallace A., Williams P., Stewart G. S. A. B. and Grierson D. (1999), Plants genetically modified to produce *N*-acylhomoserine lactones communicate with bacteria. Nature Biotechnol. **17**, 1017–1020.

Gamblin S. J., Davies G. J., Grimes J. M., Jackson R. M., Littlechild J. A. and Watson H.C. (1991), Activity and specificity of human aldolase. J. Mol. Biol. **219**, 573–576.

Haake V., Zrenner R., Sonnewald U. and Stitt M. (1998), A moderate decrease of plastid aldolase activity inhibits photosynthesis, alters the levels of sugars and starch, and inhibits growth of potato plants. Plant J. **14**, 147–157.

Hartman F. C. and Barker R. (1965), An exploration of the active site of aldolase using structural analogs of fructose diphosphate. Biochemistry **4**, 1068–1075.

Jin H., Hartman G. L., Nickell C. D. and Widholm J. M. (1996), Characterization and purification of a phytotoxin produced by *Fusarium solani*, the causal agent of soybean sudden death syndrome. Phytopathology **86**, 277–282.

Krüger I. and Schnarrenberger C. (1983), Purification, subunit structure and immunological comparison of fructose-bisphosphate aldolases from spinach and corn leaves. Eur. J. Biochem. **136**, 101–106.

Lebherz H. G., Leadbetter M. M. and Bradshaw R. A. (1984), Isolation and characterization of the cytosolic and chloroplast forms of spinach leaf fructose diphosphate aldolase. J. Biol. Chem. **259**, 1011–1017.

Marshall J. J., Wilson K. J. and Lebherz H. G. (1989) Structural similarities between spinach chloroplast and cytosolic class I fructose-1,6-bisphosphate aldolases. Plant Physiol. **91**, 1393–1401.

Morrell S. and Rees T. (1986), Sugar metabolism in developing tubers of *Solanum tuberosum*. Phytochemistry **25**, 1579–1585.

Pedras M. S. C., Zaharia I. L., Gai Y., Zhou Y. and Ward D. E. (2001), *In planta* sequential hydroxylation and glycosylation of a fungal phytotoxin: Avoiding cell death and overcoming the fungal invader. Proc. Natl. Acad. Sci. USA **98**, 747–752.

Pelzer-Reith B., Penger A. and Schnarrenberger C. (1993), Plant aldolase: cDNA and deduced amino-acid sequences of the chloroplast and cytosol enzyme from spinach. Plant Mol. Biol. **21**, 331–340.

Sali A., Potterton L., Yuan F., Van Vlijmen H. and Karplus M. (1995), Evaluation of comparative protein modeling by MODELLER. Proteins **23**, 318–326.

Staskawicz R. J., Mudgett M. B., Dangl J. L. and Galan J. E. (2001), Common and contrasting themes of plant and animal diseases. Science **292**, 2285–2289.

Tanaka T., Hanato K., Watanabe M. and Abbas H. K. (1996), Isolation, purification and identification of 2,5-anhydro-D-glucitol as a phytotoxin from *Fusarium solani*. J. Nat. Tox. **5**, 317–329.

Vera-Estrella R., Barkla B. J., Higgins V. J. and Blumwald E. (1994), Plant defense response to fungal pathogens. Plant Physiol. **104**, 209–215.